ACS Sustainable Chemistry & Engineering

Research Article

pubs.acs.org/journal/ascecg

One-Step Conversion of Biomass-Derived 5-Hydroxymethylfurfural to 1,2,6-Hexanetriol Over Ni–Co–Al Mixed Oxide Catalysts Under Mild Conditions

Shengxi Yao,[†] Xicheng Wang,[†] Yijun Jiang,[†] Feng Wu,[†] Xinguo Chen,[†] and Xindong Mu*[,†,‡]

[†]CAS Key Laboratory of Bio-based Materials, Qingdao Institute of Bioenergy and Bioprocess Technology, Chinese Academy of Sciences, Qingdao 266101, P.R. China

[‡]Qingdao Engineering Research Center for Biomass Green Chemical Conversion, Qingdao 266101, P.R. China

Supporting Information

ABSTRACT: The conversion of biomass-derived 5-hydroxymethylfurfural (HMF) was examined over Ni–Co–Al mixed oxide catalysts derived from corresponding hydrotalcite-like compounds (HTlcs). 1,2,6-Hexanetriol (1,2,6-HT) was obtained in 64.5% yield under mild reaction conditions. The catalysts were characterized by X-ray powder diffraction (XRD), CO_2 temperature-programmed desorption (CO_2–TPD), N_2 physical adsorption, and H_2 temperature-programmed reduction (H_2–TPR), and the reaction product distribution was correlated with the catalyst composition and reaction conditions. The reaction pathway was proposed based on the results. In all cases, the conversion of HMF proceeds according to a pathway that begins with the aldehyde group being hydrogenated to form 2,5-dihydroxymethylfuran (2,5-DHF). This product then undergoes a ring-opening reaction to form 1,2,6-HT. A synergetic effect between Ni and Co was observed, which significantly promoted catalytic activity and selectivity.

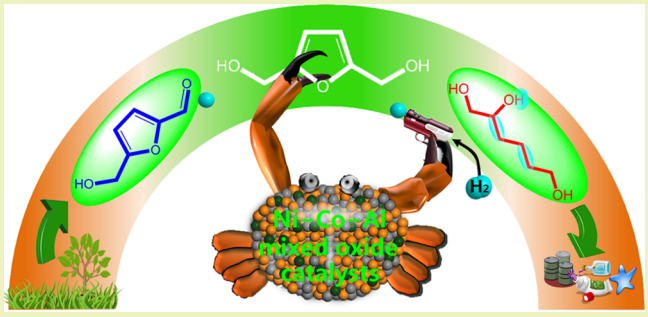

KEYWORDS: *5-Hydroxymethylfurfural, 1,2,6-Hexanetriol, Mixed metal oxide catalyst, NiO, CoO, Furan derivatives*

INTRODUCTION

Biomass refinery is of great significance for the sustainable development of human society and requires efficient methods to convert carbohydrates into various chemical compounds.[1] 1,2,6-Hexanetriol (1,2,6-HT) is an important commodity chemical or intermediate that can be used as a humectant, solvent, and viscosity-controlling agent in medicaments, cosmetics and the resins/plastics industries[2−4] or as a precursor to produce 1,6-hexanediol (1,6-HDO) and 1,2-hexanediol (1,2-HDO).[5] 1,2,6-HT is currently produced from the dimerization of oil-based acrolein, followed by complex hydrolysis and hydrogenation.[6,7] Thus, to simplify the process and to increase sustainability, it is desirable to design a novel process for the direct conversion of bio-based renewable feedstocks into 1,2,6-HT.

5-Hydroxymethylfurfural (HMF) is a key intermediate because of its rich functionality and easy availability, being derived from carbohydrates such as hexoses or even cellulose.[1] Commonly, the conversion of HMF into value-added alkyl diols and triols involves a catalytic ring-opening process for the furan or tetrahydrofuran ring (Scheme 1). In previous reports, high pressure and high catalyst loading[8−13] were usually required for the selective ring opening of the tetrahydrofuran ring to give diols. Although relatively mild reaction conditions were also successfully applied for the opening of the furan ring,[14] the selectivity of the targeted diols was low (approximately 30%). A multi-step process[15] involving the hydrogenation of the furan ring followed by the ring opening of the tetrahydrofuran was needed to achieve a high selectivity of diols from HMF. Thus, it is still necessary to improve the

Scheme 1. Reaction Pathways for Conversion of HMF

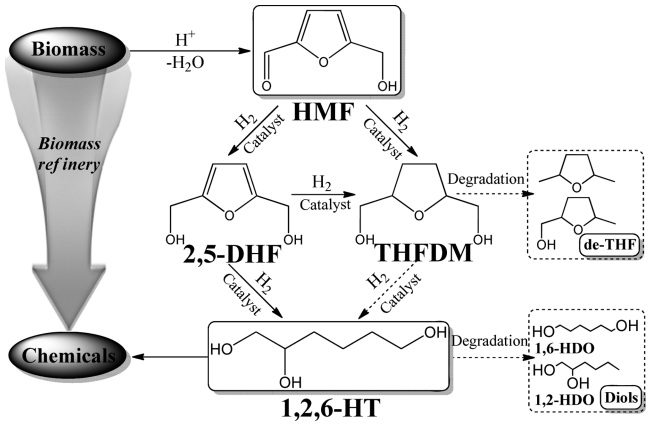

Received: June 17, 2013
Published: October 1, 2013

process for the sustainable conversion of HMF. Zhang et al.[16] provided us with a new strategy for targeting other valuable diols or triols (e.g., 1,2-PDO), not just 1,5-PDO, from the ring-opening reaction of furfural alcohol and other furan derivatives. Herein, we present a new sustainable process for the direct conversion of HMF to 1,2,6-HT in a yield of 64.5% under relatively mild conditions.

Mixed oxide catalysts derived from the heat treatment of hydrotalcite-like compounds (HTlcs) often display advantageous properties, including a homogeneous microstructure, enhanced metal-oxide interactions, high specific surface area, and strong basic properties.[17,18] In this study, we report the observation that easily prepared Ni−Co−Al mixed oxide catalysts derived from HTlcs can effectively catalyze the conversion of HMF to 1,2,6-HT under mild reaction conditions. A synergetic effect between Ni and Co greatly enhances the reaction activity and product selectivity.

EXPERIMENTAL SECTION

Materials and Chemicals. HMF (99% purity) was obtained from Wujiang Yingchuang Chemical Reagent Co., Ltd. Analytical grade $Co(NO_3)_2{\cdot}6H_2O$, $Ni(NO_3)_2{\cdot}6H_2O$, $Al(NO_3)_3{\cdot}9H_2O$, NaOH, and Na_2CO_3 were purchased from Sinopharm Chemical Reagent Co., Ltd., and used without further purification.

Catalyst Preparation. Ni−Co−Al mixed oxide catalysts (with the (Ni + Co)/Al molar ratio fixed at 3 and Ni/Co from 0 to 1) were synthesized by a co-precipitation method described in previous reports.[14,19] In detail, a volume of distilled water was placed in a reaction vessel at room temperature (RT), and a mixed aqueous solution of nickel, cobalt, and aluminum nitrates (0.12 M) and the base solution (0.1 M, with $NaOH/Na_2CO_3 = 2$) were added dropwise into the distilled water at RT under vigorous stirring to maintain the pH value approximately 10, and then the resultant slurry was aged in the mother liquor at 80 °C for 20 h. After cooling to RT, the solid precipitate was washed thoroughly with deionized water until the pH value of the filtrate was approximately 7. The filter cake was dried at 100 °C in air for 12 h (HTlcs) and then underwent a calcination at 400 °C for 4 h (5 °C min^{-1}) in air (calcined samples) and a reduction at 500 °C (pure hydrogen at 50 mL min^{-1}) for another 4 h. Before exposure to air, the samples were passivated in a 1% O_2/N_2 flow for 2 h at RT (reduced samples).

Reactivity Studies. Activity tests were performed in a 300 mL mechanically stirred Parr 4560 series autoclave equipped with a 4843 PID temperature controller. In a typical experiment, 1 g of HMF dissolved in 100 mL of methanol and 0.2 g of catalyst was loaded before sealing the reactor. The autoclave was purged with H_2 three times to drive out the air and then brought to an appropriate pressure at RT. Finally, the reactor was rapidly heated (without stirring) to the desired reaction temperature (defined as zero time), and the reaction was carried out for a chosen time at a stirring speed of 600 rpm.

Recycling experiments of the solid catalyst were carried out in a similar manner but after removing the liquid solution by filtration. The solid catalyst was simply washed with methanol and dried at 40 °C for 8 h and then introduced into the autoclave together with fresh HMF solution for a subsequent catalytic cycle.

The conversion of HMF and selectivity and yield of the products were defined on carbon basis calculations, as shown in the formulas listed below. The mass balance for each result was confirmed by repeated tests, and the differences in the mass balance were always in the range of the experimental error (<2%).

$$\text{Conversion (\%)} = \frac{\text{moles of HMF consumed}}{\text{moles of HMF initially consumed}} \times 100$$

$$\text{Selectivity (\%)} = \frac{\text{moles of carbon in specific product}}{\text{moles of carbon in consumed HMF}} \times 100$$

$$\text{Yield (\%)} = [\text{Conversion (\%)} \times \text{Selectivity (\%)}]/100$$

Characterization Techniques. The metal contents in the samples and metal leaching were analyzed by inductively coupled plasma-atomic emission spectroscopy (ICP-AES, Thermo Elemental, IRIS Intrepid II XSP). Solid samples were dissolved in aqua regia and diluted before measurement.

X-ray powder diffraction (XRD) patterns of the HTlcs and the calcined and reduced samples were recorded at RT on a Bruker D8 Advance powder diffractometer employing Cu Kα radiation (40 kV, 40 mA) with a scanning speed (2θ) of 4° min^{-1}.

Temperature programmed reduction (TPR) analyses were performed with a Micromeritics AutoChem II Chemisorption Analyzer. Approximately 100 mg of each sample was placed in quartz reactors and reduced in a stream of 20 mL min^{-1} H_2 (10 vol% in Ar) at a heating rate of 10 °C min^{-1}.

Nitrogen adsorption and desorption isotherms of the samples were measured at −196 °C with a Micromeritics ASAP 2020 apparatus. BET surface areas were calculated using the desorption isotherms. All samples were outgassed at 250 °C for 10 h before measurement.

The alkalinity of the catalysts was measured by the temperature-programmed desorption of CO_2 (TPD). Samples were pretreated in a flow of N_2 at 300 °C for 2 h, cooled to 50 °C, and then exposed to a flowing mixture of 10% CO_2 in N_2 until the surface saturation was achieved (30 min). Then, the temperature was raised from 50 to 800 °C at a rate of 10 °C min^{-1} in N_2, and the desorbed products were monitored by a TCD detector.

Product Analysis. Products were filtered through a membrane filter (0.22 μm pore size) prior to analysis. The products were quantified using a gas chromatograph (Varian 450-GC) equipped with a flame ionization detector (FID) and a Galaxy workstation. The GC column used was a DB-FFAP column (30 m × 0.25 mm × 0.25 μm) manufactured by Agilent.

The product analysis was also confirmed by gas chromatography−mass spectrometry (GC-MS) carried out using gas chromatography (GC, 7890A, Agilent, U.S.A.) coupled with mass spectrometry (MS, 5975C, Agilent, U.S.A.). The GC-MS was equipped with an HP-Innowax column (30 m × 0.25 mm × 0.25 μm).

RESULTS AND DISCUSSION

Catalyst Characterization. The textural properties of the reduced samples are summarized in Table 1. The Ni/Co ratios calculated from the ICP-AES results are also presented. The results show that the partial substitution of Co by Ni does not significantly change the surface area (105.4−137.2 m^2/g), and the pore distribution indicates that mainly mesopores (13.7−20.4 nm) exist in these samples. In addition, the metal content in the HTlcs are presented in Table S1 of the Supporting Information. The experimentally determined metal molar ratios (Ni/Co and (Ni + Co)/Al) are quite similar to the values in the initial solution, suggesting complete precipitation.

Table 1. Textural Properties of the Reduced Samples

sample	Ni/Co ratio[a]	S_{BET} (m^2/g)[b]	V_p (cm^3/g)[b]	D_p (nm)[b]
3CoAl	0.00	105.4	0.593	20.4
0.3Ni2.7CoAl	0.11	111.3	0.474	14.9
0.5Ni2.5CoAl	0.20	120.6	0.513	14.2
0.9Ni2.1CoAl	0.42	124.9	0.575	15.7
1.5Ni1.5CoAl	0.97	137.2	0.617	15.3
3NiAl	−	131.1	0.489	13.7

[a]Atomic ratio was determined by ICP-AES. [b]S_{BET}: BET specific surface area. V_p: Total pore volume. D_p: Average pore diameter.

The XRD patterns (Figure 1) of the reduced samples (reduction at 500 °C and passivation at RT) show broad features of a rock salt-type phase (common to NiO and CoO and/or a NiO−CoO solid solution) and traces of a spinel

dx.doi.org/10.1021/sc4003714 | ACS Sustainable Chem. Eng. 2014, 2, 173−180

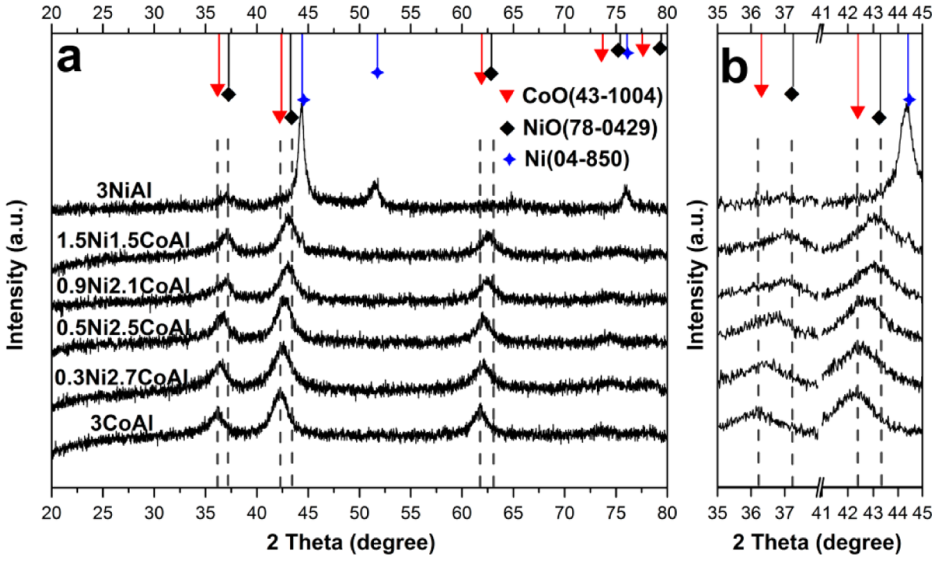

Figure 1. XRD patterns of the reduced samples.

phase. However, it is difficult to clearly distinguish the NiO and CoO physical mixture and NiO−CoO solid solution by examining their XRD patterns, which reveal poor crystallization and very similar features. With the introduction of Ni, the main reflection peaks slightly shift to higher angles (Figure 1b) owing to the gradual replacement of Co^{2+} with Ni^{2+} in the microstructures. The absence of an Al_2O_3 phase may be explained as a proper mixing of that phase within the bulk of the NiO and CoO phases. Moreover, the 3NiAl sample exhibits peaks of Ni (JCPDS 04-850) along with a NiO phase (JCPDS 78-0429), indicating that NiO was partially reduced to Ni^0 during the reduction process. However, the reduction of Ni is greatly inhibited by the introduction of Co. It can be observed that the 1.5Ni1.5CoAl sample shows only a small peak of Ni^0 (2θ = 44.5°), and no reflection of the Ni metallic phase can be detected in the samples with lower Ni/Co ratios (0.3Ni2.7CoAl and 0.5Ni2.5CoAl). This phenomenon indicates that the NiO phase strongly interacts with the CoO phase, most likely forming a NiO−CoO solid solution, which is thought to form very easily between NiO and CoO because of their similar unit cell structures.[20] The formation of a NiO−CoO solid solution made it difficult for the NiO to be reduced to Ni^0. Only a small amount of well-dispersed NiO can be reduced to some easily reducible Ni species, which may not be reflected in the XRD patterns. A similar phenomenon was also observed by Hu[21] when reducing a NiO/CoO−MgO solid solution.

The XRD patterns of the HTlcs and calcined samples are also shown in Figure S1 of the Supporting Information. The HTlcs (Figure S1a, Supporting Information) exhibit a single hydrotalcite-like structure without co-crystallization of a discrete impurity phase. The well-defined (110) and (113) diffraction peaks reveal a good dispersion of the metal ions (Ni^{2+}, Co^{2+}, and Al^{3+}) in the hydroxide layers.[22] The calcined samples (Figure S1b, Supporting Information) show diffraction peaks corresponding to a typical spinel-like phase. The poor crystallization of these phases is favorable for the reduction to metal oxides and even metallic Ni.

The nitrogen adsorption−desorption isotherms of the 0.5Ni2.5CoAl sample are displayed in Figure 2. The sample presents a type IV adsorption isotherm, according to the IUPAC classification. Two uptakes at a relative pressure of 0.4−

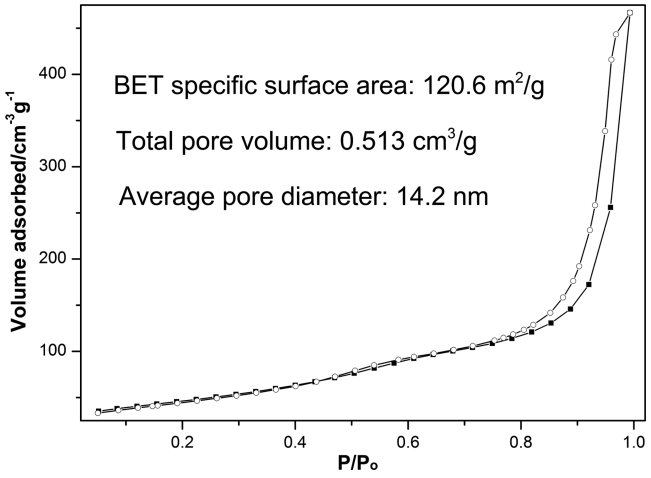

Figure 2. N_2 adsorption−desorption isotherms of the 0.5Ni2.5CoAl sample.

0.6 and 0.8−1.0 correspond to the mesopores and the voids of the interparticle spaces, respectively.[23] In addition, the average pore diameter of 14.2 nm indicates a mesopore structure. Xu[23] declared that the oxidation of Co^{2+} to Co^{3+} during the CoAl-HT calcination process is critical for the formation of the mesopore structure, as the change of the coordination state (Co^{2+} to Co^{3+}) resulted in the reorganization of the inner structure with the interlayer space almost opened (mesopores formed). We also observed that the mesopore structure remained after the reduction.

HTlc-derived mixed oxides usually have specific surface alkalinity, which may influence the cleavage of C−O bonds. CO_2−TPD profiles (Figure 3) are presented to show the alkalinity of our samples. The intensity and number of the basic sites on the surface are categorized according to their peak positions (desorption temperature) and peak areas. Three desorption peaks are seen, corresponding to weak (OH^- groups, approximately 100 °C), moderate (M−O pairs, 150−200 °C), and strong basic sites (O^{2-} pairs, approximately 450 °C). With the introduction of Ni (from 3CoAl to 3NiAl), the peak positions of the moderate basic sites are changed, whereas the peak positions of the weak and strong basic sites remain

dx.doi.org/10.1021/sc4003714 | ACS Sustainable Chem. Eng. 2014, 2, 173−180

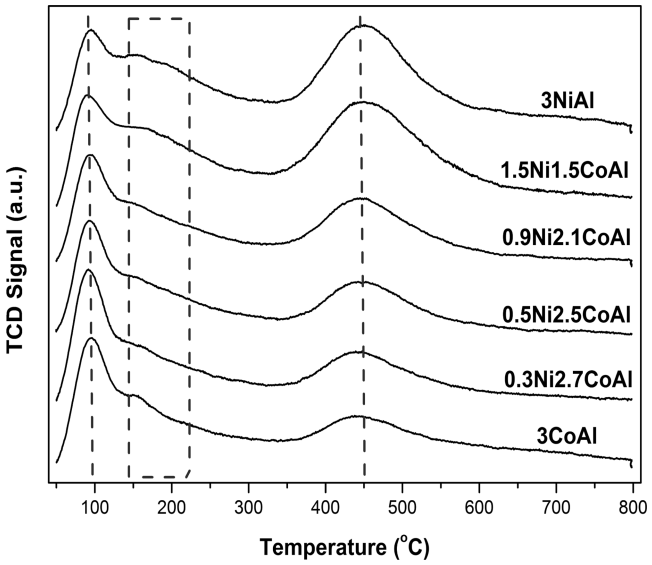

Figure 3. CO_2–TPD patterns of the reduced samples.

constant. Furthermore, the number of weak sites increases, and the number of strong sites decreases with the introduction of Ni. However, the number of moderate sites is difficult to identify and quantify because of peak overlap.

The H_2–TPR profiles for the calcined (Figure 4a) and reduced (Figure 4b) samples are also presented. For the calcined samples, 3CoAl shows a two-stage reduction. The peak in the lower temperature range (300–400 °C) can be attributed to the reduction of Co^{3+} to Co^{2+}, and the peak above 650 °C can be assigned to the reduction of a Co^{2+}–Al^{3+}-like phase, which behaves similarly to $CoAl_2O_4$ spinel.[23−26] A

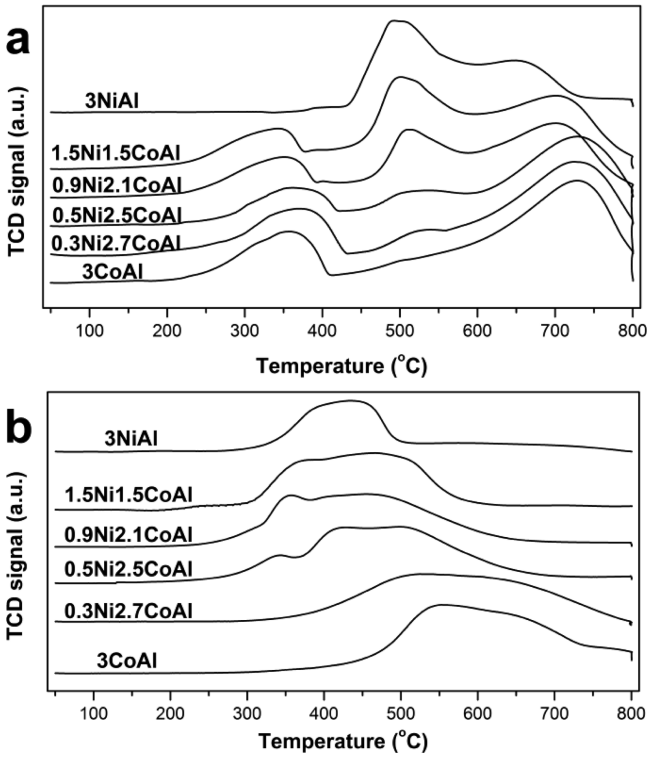

Figure 4. H_2–TPR patterns of the calcined (a) and reduced (b) samples.

third reduction peak (450–600 °C) appears with the introduction of Ni, and the peak intensity increases along with the nickel loading, indicating a single-stage reduction of the poorly crystallized nickel spinel ($NiAl_2O_4$ and $(Ni,Co)_2AlO_4$) to the oxides phase (NiO or NiO–CoO solid solution) and metallic phase (Ni^0). A similar reduction peak at 490 °C, corresponding to the reduction of $NiAl_2O_4$ to NiO and Ni^0, is also observed in the 3NiAl profile. On the basis of these results, we chose 500 °C as the optimal reduction temperature to control the reduction degree of the nickel oxides. In addition, Figure 4b shows the H_2–TPR profiles of the reduced catalysts. Broad peaks are observed for all the samples, indicating a multistage reduction. The 3CoAl sample shows a broad peak that can be ascribed to the reduction of well-dispersed CoO and CoO interacting with the $CoAl_2O_4$ spinel. The broad peak of the 3NiAl sample includes the reduction of the dispersed NiO and NiO in contact with the support. Other reduced samples (Ni/Co from 1/9 to 1/1) exhibit a large broad peak, possibly corresponding to the reduction of well-dispersed NiO (approximately 350 °C), bulk NiO (350–500 °C), and bulk CoO (approximately 500–600 °C). The first peak (approximately 350 °C) can also be assigned to the easily reducible Ni species (as inferred in the XRD discussion), which were oxidized during the passivation process. Moreover, there is a trend of the reduction peak gradually decreasing to a lower temperature with an increasing Ni/Co ratio, indicating a close interaction between the Ni and Co species. This behavior was also observed by Marco et al.[27]

Catalytic Reactions of HMF. The mass balances of carbon estimated by summing the detected products and unreacted HMF vs fed HMF are approximately 70–98%. The mass losses are ascribed to the formation of polymers and/or cokes.[1] The desired product from the catalytic ring opening of HMF is 1,2,6-HT. Other identified products (Scheme 1) include 2,5-dihydroxymethylfuran (2,5-DHF), 2,5-THF-dimethanol (THFDM), 1,2-HDO, 1,6-HDO, (2-hydroxymethyl-5-methyl)-tetrahydrofuran (HMTHF), and 2,5-bis(methyl)-tetrahydrofuran (BMTHF). HMTHF and BMTHF are formed by the C–O bond cleavage of THFDM and are recorded as de-THF for short.

HMF Conversion Over Different Catalysts and Reaction Mechanism. First, commercial Raney Ni and Raney Co (Table 2, entries 1 and 2) were used for the HMF conversion. Both catalysts showed good activity in hydrogenating the furan ring (forming THFDM) but almost no activity for the ring opening. These results indicated that the single metal Ni or Co was not responsible for the hydrogenolytic ring opening of HMF under mild conditions. Furthermore, solid base catalysts were used to inhibit the formation of levulinic acid, which was produced easily using an acidic catalyst.[1] Using 3CoAl (entry 3) resulted in 2,5-DHF as the main product (83.0%) together with a low production of THFDM (4.1%), indicating that the hydrogenation capability of the 3CoAl catalyst was sufficient to saturate the aldehyde but insufficient for the furan ring. To improve the hydrogenation activity, Ni was introduced, forming various Ni–Co–Al mixed oxide catalysts (entries 4– 7). As expected, the hydrogenation capability of the catalysts was enhanced considerably, especially for the 1.5Ni1.5CoAl (entry 7, Ni/Co = 1), over which HMF was quickly converted to the fully hydrogenated THFDM with a yield of 89.0%, which was even higher than the result (81.1%) achieved with 3NiAl (entry 8). Interestingly, increasing the Ni/Co ratio led to a rise followed by a fall in the product yield,

dx.doi.org/10.1021/sc4003714 | ACS Sustainable Chem. Eng. 2014, 2, 173–180

Table 2. Results of the Hydrogenolytic Ring Opening of HMF[a]

			yield based on carbon (%)						
entry	sample	conv.	1,2-HDO	1,6-HDO	de-THF	THFDM	2,5-DHF	1,2,6-HT	sum
1	Raney Ni	100	0	0	0	92.0	0	0	92.0
2	Raney Co	100	0	0	0	95.8	0	1.3	97.1
3	3CoAl	89.4	0	0	0	4.1	83.0	0	87.1
4	0.3Ni2.7CoAl	100	3.2	0.6	0.1	11.7	59.7	14.8	90.1
5	0.5Ni2.5CoAl	100	2.2	0	0	12.5	40.4	37.4	92.5
6	0.9Ni2.1CoAl	100	0.9	0.4	0.1	38.8	23.4	23.3	86.9
7	1.5Ni1.5CoAl	100	0	0	0.2	89.0	2.1	0	91.3
8	3NiAl	95.4	0	0	0.2	80.1	13.2	0	93.5
9	Raney Ni+3CoAl[b]	100	0	0	0.1	89.8	0.3	0	90.2
10	3NiAl+3CoAl[b]	92.6	0	0	0	28.1	61.3	0	89.4

[a]Conditions: 0.2 g of catalyst, 1 g of HMF in 100 mL methanol, 120 °C, 4 MPa of H_2, and 4 h. [b]Catalyst weight ratio: Raney Ni (or 3NiAl):3CoAl = 1:5.

reaching a maximum over the 0.5Ni2.5CoAl catalyst (Ni/Co = 0.2). This phenomenon is difficult to explain because of the similar surface area, pore volume, pore diameter, or alkalinity; thus, we suppose that a crucial cooperation between Ni and Co may be responsible for the ring opening.

To verify the existence of a synergetic effect, the physical mixtures of 3CoAl with Raney Ni and with 3NiAl catalysts were also tested (entries 9 and 10). As expected, HMF was converted to its hydrogenation products (2,5-DHF and THFDM), but no ring-opening products were observed. Our results (entries 3− 10) revealed that most of the Ni−Co−Al mixed oxide catalysts showed catalytic ring-opening activity, in contrast to 3NiAl and 3CoAl and their physical mixture. This finding can most likely be ascribed to a mutual interaction and synergetic effect between the CoO and NiO species, as shown by the XRD and H_2−TPR results. On the basis of a previous report,[14] CoO is mainly responsible for the adsorption of the furan ring and C−O bond cleavage, while the Ni site catalyzes hydrogenation. The cooperation between the Co and Ni species provides a synergetic effect to catalyze the ring opening of the furan. However, this cooperation requires a proper interaction between the Ni and Co active sites and an appropriate ratio of Ni/Co to balance the C−O cleavage and subsequent hydrogenation. Indeed, an interaction between the Ni and Co species was demonstrated by the XRD and H_2−TPR results, and the difference of the Ni/Co ratio was certified by the ICP-AES results. The 0.5Ni2.5CoAl catalyst (entry 5, Ni/Co = 0.2) exhibited the best ring-opening activity. However, a low ring-opening activity was observed for both the lower (entries 3 and 4) and higher (entries 7 and 8) Ni/Co ratio catalysts, which indicated that lower Ni/Co ratios in the catalysts do not provide enough Ni−Co−O sites and that higher Ni/Co ratios in the catalysts supply numerous hydrogenation sites (Ni^0), which quickly hydrogenate the intermediate (step 2 in Scheme 2) to THFDM and greatly inhibit the ring-opening process (entry 7).

Considering our experimental results in the present work and the reported mechanisms in the existing literature,[14,16,28,29] a reaction mechanism for the ring opening of HMF to 1,2,6-HT is proposed (Scheme 2). First, the aldehyde group is quickly hydrogenated to form 2,5-DHF (step 1). Then, the furan ring in the 2,5-DHF molecule may be adsorbed in two different modes: parallel (a) and tilted (b). The former may lead to complete hydrogenation, forming THFDM, while the latter may generate a key semi-hydrogenation intermediate (B1), leading to the ring opening through the C−O bond cleavage

Scheme 2. Proposed Reaction Mechanism for the One-Step Conversion of HMF

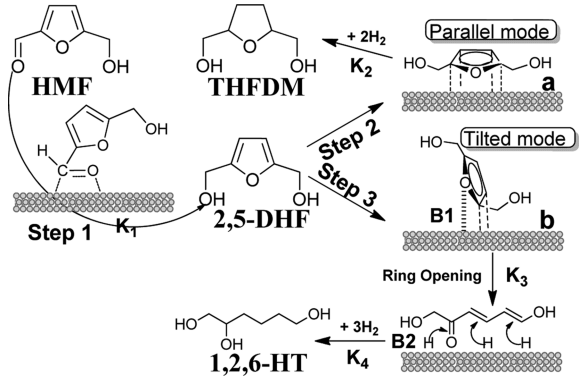

with the formation of B2. Subsequently, the hydrogenation of B2 occurs to give 1,2,6-HT.

As mentioned previously, CoO provides adsorption sites for the tilted adsorption, and Ni was responsible for the hydrogenation of B2 (Scheme 2). However, Ni was also active in the hydrogenation of 2,5-DHF to THFDM. Thus, the amount of Ni should be adjusted to a proper value to match the amount of Co to improve the ring-opening selectivity. We determined that the 0.5Ni2.5CoAl possessed a more suitable Ni/Co ratio than the other samples, and thus, it showed the best ring-opening activity. Moreover, Zhang et al.[16] believed that Mn^{2+} might stabilize the intermediate B1 to suppress the complete hydrogenation of the furan ring, and we infer that the Co^{2+} in our catalysts may have the same effect, weakening the hydrogenation ability of Ni.

Effects of the Reaction Temperature. The effect of the reaction temperature on the hydrogenolytic ring opening of HMF is summarized in Figure 5. A longer reaction time (8 h) was used to further transform 2,5-DHF to the desired product. At a temperature of 100 °C, the main products were 2,5-DHF (54.2%) and THFDM (34.4%), with other products present in a negligible amount. When the reaction was performed at 120 °C, the yield of 1,2,6-HT increased gradually, in contrast to the yield of 2,5-DHF and THFDM. This result revealed that the ring opening of the furan may not happen below 100 °C, but it was significantly accelerated by increasing the reaction temperature. Further increasing the reaction temperature (140 to 160 °C) led to a remarkable decrease in the 1,2,6-HT yield (41.9% to 20.1%) but almost no change in the

dx.doi.org/10.1021/sc4003714 | ACS Sustainable Chem. Eng. 2014, 2, 173−180

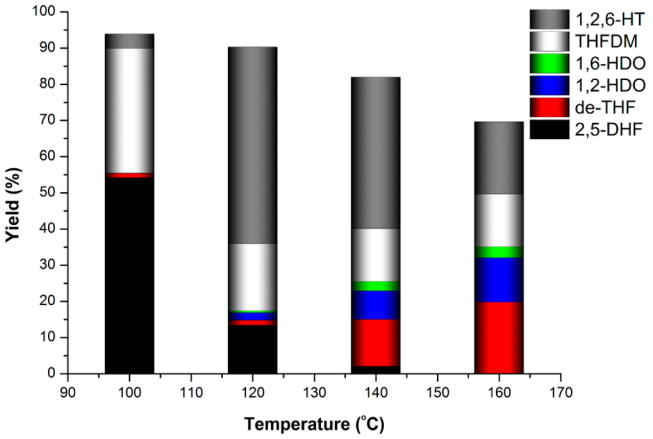

Figure 5. Effect of reaction temperature. Conditions: 0.2 g of 0.5Ni2.5CoAl, 1 g of HMF in 100 mL methanol, 4 MPa of H_2, and 8 h.

THFDM yield (14.6% to 14.5%). This result does not necessarily mean that the THFDM did not degrade at the increased temperature; it is possible that the amount of THFDM generated (from 2,5-DHF) and the amount of THFDM degraded (to de-THF) were almost equal. In other words, as shown in Scheme 3, when increasing the temperature

Scheme 3. Reaction Pathways in the Conversion of 2,5-DHF

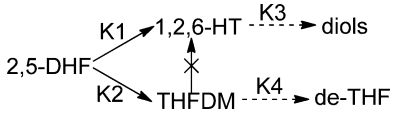

from 140 to 160 °C, all the kinetic parameters increased with the following trend: K2∼K4 > K3≫K1. As a result, more 2,5-DHF was converted to THFDM, and more THFDM was degraded to de-THF. However, the amount of THFDM remained roughly constant. Moreover, the total yield of detected products decreased significantly from 82.0% to 69.7% at the increased temperature. The GC-MS results showed that the C−O bond cleavage products were mainly 1,2-HDO, 1,6-HDO, HMTHF and BMTHF. Some heavy constituents (Figures S2−S6, Supporting Information) were also detected, which might be responsible for the C unbalance. These results also indicated that high temperature accelerated the rate of degradation and polymerization.

On the basis of the above results, we concluded that 1,2,6-HT was formed by the ring opening of 2,5-DHF. This process reached the highest yield at 120 °C over the 0.5Ni2.5CoAl catalyst. Therefore, 120 °C was the optimal temperature for the ring opening of HMF in this reaction system. At this temperature, the yield of 1,2,6-HT reached 54.4% and that of THFDM was controlled at 18.5%.

Effects of the Reaction Time. A typical profile of this reaction is shown in Figure 6. At the initial stage of the reaction (0.5 h), HMF was quickly converted to 2,5-DHF with a selectivity over 97%, and then 2,5-DHF was further transformed into other products. At a reaction time of 2 h, HMF was fully converted into 2,5-DHF with a yield of 70.5%, which is in agreement with previously reported results.[30] Increasing the reaction time to 4 h, 2,5-DHF was quickly turned into THFDM and 1,2,6-HT, leading to overall yields of 12.5% and 37.4%, respectively. After increasing the reaction time to 8 h, 1,2,6-HT

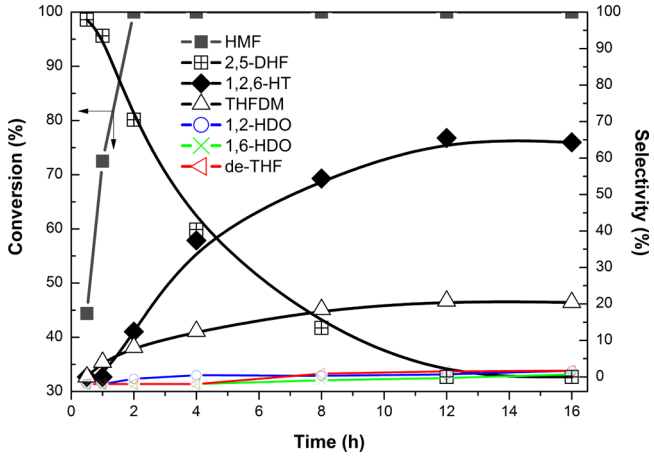

Figure 6. Effect of the reaction time. Conditions: 0.2 g of 0.5Ni2.5CoAl, 1 g of HMF in 100 mL methanol, 120 °C, and 4 MPa of H_2.

was produced in a higher yield (54.4%), while the THFDM yield smoothly increased to 18.5%. When the reaction time reached 12 h, the yield of 1,2,6-HT reached the highest value of 64.5%, whereas the amount of 2,5-DHF decreased to a negligible level. After complete hydrogenation, a longer reaction time (i.e., 16 h) did not significantly change the product distribution; THFDM remained at an almost constant yield in the 20% range, indicating that THFDM could not be converted into 1,2,6-HT through ring opening in our reaction system.

Over the entire time span of 1−16 h and at the fixed reaction temperature of 120 °C, the yield of THFDM remained almost constant, whereas the yield of 1,2,6-HT increased sharply at the expense of 2,5-DHF. This phenomenon suggested that 1,2,6-HT was formed directly from the ring opening of 2,5-DHF.

Effects of the Reaction Pressure. Figure 7 shows the influence of the initial H_2 pressure on the yield of the products.

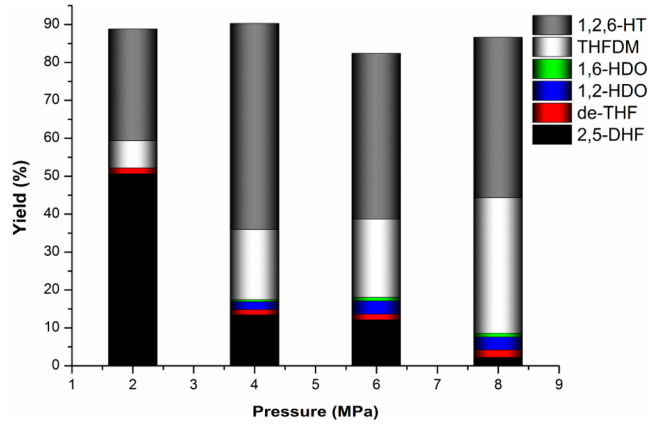

Figure 7. Effect of the reaction pressure. Conditions: 0.2 g of 0.5Ni2.5CoAl, 1 g of HMF in 100 mL methanol, 120 °C, and 8 h.

In detail, a rapid increase in the 1,2,6-HT yield vs conversion of 2,5-DHF occurred when the H_2 pressure was elevated from 2 to 4 MPa, indicating that 2,5-DHF was largely converted to 1,2,6-HT at a relatively moderate pressure (4 MPa). Comparing the reactions carried out at 4 and 6 MPa, the conversion of 2,5-DHF and the yield of the THFDM did not change notably, but the yield of 1,2,6-HT and the C balance slightly decreased with

dx.doi.org/10.1021/sc4003714 | ACS Sustainable Chem. Eng. 2014, 2, 173−180

an increase in pressure. This phenomenon could be explained as the accelerated degradation and polymerization of 1,2,6-HT, indicating that higher pressure was not favorable for producing 1,2,6-HT. Moreover, THFDM was favored at high pressure based on the results obtained at 6 and 8 MPa. As mentioned previously, the hydrogenation ability of CoO was too weak to saturate the furan ring. However, under high H_2 pressure, CoO might have adsorbed more hydrogen atoms, which hydrogenated the furan ring and formed THFDM. Therefore, a moderate pressure of 4 MPa was preferred to maintain the reaction activity and inhibit the complete hydrogenation of the furan ring.

On the basis of the influence of the reaction conditions on the yield of 1,2,6-HT, we chose a reaction temperature of 120 °C, an initial H_2 pressure of 4 MPa, and a reaction time of 12 h as the optimal conditions for the selective production of 1,2,6-HT from HMF. We assumed that the reaction pathway proceeded as indicated in Scheme 1, with both aldehyde and furan ring groups. HMF was initially quickly hydrogenated to 2,5-DHF and subsequently converted to 1,2,6-HT or THFDM based on the adsorption mode of the furan ring (tilted or parallel, Scheme 2). However, these products could be further hydrogenated into 1,2-HDO, 1,6-HDO, HMTHF, and BMTHF.

Catalyst Recyclability. To investigate the recyclability of the catalyst, a batch of the 0.5Ni2.5CoAl was used in repeated runs under the optimal conditions for the selective production of 1,2,6-HT from HMF. As shown in Figure 8, the catalyst

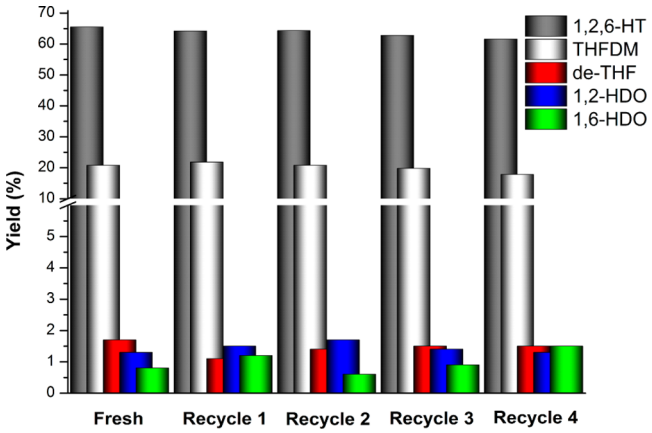

Figure 8. Reusability of the 0.5Ni2.5CoAl catalyst for the hydrogenolytic ring opening of HMF. Conditions: 0.2 g of 0.5Ni2.5CoAl, 1 g of HMF in 100 mL methanol, 120 °C, 4 MPa of H_2, and 12 h.

could be reused at least four times with little loss of activity. Almost the same yields of detected products, including 1,2,6-HT and THFDM, were obtained after four cycles.

To prove that the reaction was catalyzed heterogeneously and to exclude the possibility of leaching and homogeneous catalysis, a test with 0.5Ni2.5CoAl catalyst was repeated in the same reaction conditions as those of entry 5 in Table 2. After 4 h, the heating jacket was immediately disassembled, and the cooling water system was opened to instantly stop the reaction. The solid catalyst was removed through filtration, while the liquid was retested for another 12 h. No further reaction was observed. ICP-AES analysis of the final reaction solution in each catalyst cycle (Figure 8) showed that only trace amounts of nickel, cobalt, and aluminum were leached (below 0.001% for the Ni^{2+}, Co^{2+}, and Al^{3+} ions in the liquid solution after reaction, which accounts for a very small percentage (below 0.025%) of the initial metal content in the solid catalyst). This limited metal leaching did not lead to a visible deactivation in the first four cycles, as shown by the recycling experiment.

CONCLUSION

In summary, Ni−Co−Al mixed metal oxides were employed as effective catalysts for the one-step conversion of HMF to 1,2,6-HT. It was demonstrated that the cooperation between the Co and Ni species provides a synergetic effect for the adsorption and catalytic ring opening of the furan ring, which significantly influences the reaction activity and product selectivity. By optimizing the catalyst composition and reaction conditions, the yield of 1,2,6-HT reached 64.5% at 120 °C and 4 MPa. This new approach provides an effective and sustainable process for the production of 1,2,6-HT from biomass.

ASSOCIATED CONTENT

Supporting Information

Elemental composition and XRD patterns of the hydrotalcite precursors and quantitative and qualitative analysis spectra. This material is available free of charge via the Internet at http://pubs.acs.org.

AUTHOR INFORMATION

Corresponding Author

*E-mail: muxd@qibebt.ac.cn.

Notes

The authors declare no competing financial interest.

ACKNOWLEDGMENTS

This work was supported by the Natural Science Foundation of China (No. 21273260).

REFERENCES

(1) Rosatella, A. A.; Simeonov, S. P.; Frade, R. F. M.; Afonso, C. A. M. 5-Hydroxymethylfurfural (HMF) as a building block platform: Biological properties, synthesis and synthetic applications. *Green Chem.* **2011**, *13* (4), 754−793.

(2) Tess, R. W.; Harline, R. D.; Mika, T. F. 1,2,6-Hexanetriol in alkyd resins. *Ind. Eng. Chem.* **1957**, *49* (3), 374−378.

(3) Miura, Y.; Hata, M.; Yuge, M.; Numano, K.; Iwakiri, K. Allergic contact dermatitis from 1,2,6-hexanetriol in fluocinonide cream. *Contact Dermatitis* **1999**, *41* (2), 118−119.

(4) Endo, K.; Sawada, T. Control of polymer structure by a chain-transfer reaction in the radical polymerization of acrylamide by beta-mercaptopropionic acid and 1,2,6-hexanetriol trithioglycolate. *Colloid Polym. Sci.* **2001**, *279* (11), 1058−1063.

(5) Buntara, T.; Noel, S.; Phua, P.; Melián-Cabrera, I. Catalyst screening studies on the conversion of 1,2,6-hexanetriol to 1,6-hexanediol. *Top. Catal.* **2012**, *55* (7−10), 612−619.

(6) Schirmann, J. P.; Weiss, F.; Benite, P. Process for the preparation of 1,2,6-hexanetriol. U.S. Patent 3773842, 1973.

(7) Liu, L.; Ye, X. P.; Bozell, J. J. A comparative review of petroleum-based and bio-based acrolein production. *ChemSusChem* **2012**, *5* (7), 1162−1180.

(8) Nakagawa, Y.; Tomishige, K. Production of 1,5-pentanediol from biomass via furfural and tetrahydrofurfuryl alcohol. *Catal. Today* **2012**, *195* (1), 136−143.

(9) Koso, S.; Nakagawa, Y.; Tomishige, K. Mechanism of the hydrogenolysis of ethers over silica-supported rhodium catalyst modified with rhenium oxide. *J. Catal.* **2011**, *280* (2), 221−229.

(10) Koso, S.; Furikado, I.; Shimao, A.; Miyazawa, T.; Kunimori, K.; Tomishige, K. Chemoselective hydrogenolysis of tetrahydrofurfuryl alcohol to 1,5-pentanediol. *Chem. Commun.* **2009**, *15*, 2035−2037.

(11) Chen, K.; Koso, S.; Kubota, T.; Nakagawa, Y.; Tomishige, K. Chemoselective hydrogenolysis of tetrahydropyran-2-methanol to 1,6-hexanediol over rhenium-modified carbon-supported rhodium catalysts. *ChemCatChem* **2010**, *2* (5), 547−555.
(12) Chen, K.; Mori, K.; Watanabe, H.; Nakagawa, Y.; Tomishige, K. C-O bond hydrogenolysis of cyclic ethers with OH groups over rhenium-modified supported iridium catalysts. *J. Catal.* **2012**, *294* (0), 171−183.
(13) Chia, M.; Pagán-Torres, Y. J.; Hibbitts, D.; Tan, Q.; Pham, H. N.; Datye, A. K.; Neurock, M.; Davis, R. J.; Dumesic, J. A. Selective hydrogenolysis of polyols and cyclic ethers over bifunctional surface sites on rhodium-rhenium catalysts. *J. Am. Chem. Soc.* **2011**, *133* (32), 12675−12689.
(14) Xu, W.; Wang, H.; Liu, X.; Ren, J.; Wang, Y.; Lu, G. Direct catalytic conversion of furfural to 1,5-pentanediol by hydrogenolysis of the furan ring under mild conditions over Pt/Co_2AlO_4 catalyst. *Chem. Commun.* **2011**, *47* (13), 3924−3926.
(15) Buntara, T.; Noel, S.; Phua, P. H.; Melián-Cabrera, I.; de Vries, J. G.; Heeres, H. J. Caprolactam from renewable resources: Catalytic conversion of 5-hydroxymethylfurfural into caprolactone. *Angew. Chem., Int. Ed.* **2011**, *50* (31), 7083−7087.
(16) Zhang, B.; Zhu, Y.; Ding, G.; Zheng, H.; Li, Y. Selective conversion of furfuryl alcohol to 1,2-pentanediol over a Ru/MnO_x catalyst in aqueous phase. *Green Chem.* **2012**, *14* (12), 3402−3409.
(17) Zhou, S.; Qian, Z.; Sun, T.; Xu, J.; Xia, C. Catalytic wet peroxide oxidation of phenol over Cu−Ni−Al hydrotalcite. *Appl. Clay Sci.* **2011**, *53* (4), 627−633.
(18) Basile, F.; Benito, P.; Fornasari, G.; Vaccari, A. Hydrotalcite-type precursors of active catalysts for hydrogen production. *Appl. Clay Sci.* **2010**, *48* (1−2), 250−259.
(19) Xu, W. J.; Liu, X. H.; Ren, J. W.; Zhang, P.; Wang, Y. Q.; Guo, Y. L.; Guo, Y.; Lu, G. Z. A novel mesoporous Pd/cobalt aluminate bifunctional catalyst for aldol condensation and following hydrogenation. *Catal. Commun.* **2010**, *11* (8), 721−726.
(20) Kuboon, S.; Hu, Y. H. Study of NiO−CoO and Co_3O_4−Ni_3O_4 solid solutions in multiphase Ni−Co−O systems. *Ind. Eng. Chem. Res.* **2011**, *50* (4), 2015−2020.
(21) Hu, Y. H. Solid-solution catalysts for CO_2 reforming of methane. *Catal. Today.* **2009**, *148* (3−4), 206−211.
(22) Yu, J. B.; Jiang, Z.; Zhu, L.; Hao, Z. P.; Xu, Z. P. Adsorption/desorption studies of NO_x on well-mixed oxides derived from Co−Mg/Al hydrotalcite-like compounds. *J. Phys. Chem. B* **2006**, *110* (9), 4291−4300.
(23) Xu, W. J.; Liu, X. H.; Ren, J. W.; Liu, H. H.; Ma, Y. C.; Wang, Y. Q.; Lu, G. Z. Synthesis of nanosized mesoporous Co−Al spinel and its application as solid base catalyst. *Microporous Mesoporous Mater.* **2011**, *142* (1), 251−257.
(24) Hermes, N. A.; Lansarin, M. A.; Perez-Lopez, O. W. Catalytic decomposition of methane over M−Co−Al catalysts (M = Mg, Ni, Zn, Cu). *Catal. Lett.* **2011**, *141* (7), 1018−1025.
(25) He, L.; Berntsen, H.; Ochoa-Fernandez, E.; Walmsley, J. C.; Blekkan, E. A.; Chen, D. Co−Ni catalysts derived from hydrotalcite-like materials for hydrogen production by ethanol steam reforming. *Top. Catal.* **2009**, *52* (3), 206−217.
(26) Wang, Z. P.; Jiang, Z.; Shangguan, W. F. Simultaneous catalytic removal of NO_x and soot particulate over Co−Al mixed oxide catalysts derived from hydrotalcites. *Catal. Commun.* **2007**, *8* (11), 1659−1664.
(27) Marco, J. F.; Gancedo, J. R.; Ortiz, J.; Gautier, J. L. Characterization of the spinel-related oxides Ni(x)Co(3−x)O4 (x = 0.3, 1.3, 1.8) prepared by spray pyrolysis at 350 degrees C. *Appl. Surf. Sci.* **2004**, *227* (1−4), 175−186.
(28) Sitthisa, S.; Pham, T.; Prasomsri, T.; Sooknoi, T.; Mallinson, R. G.; Resasco, D. E. Conversion of furfural and 2-methylpentanal on Pd/SiO_2 and Pd−Cu/SiO_2 catalysts. *J. Catal.* **2011**, *280* (1), 17−27.
(29) Yan, F. Q.; Qiao, M. H.; Wei, X. M.; Liu, Q. P.; Deng, J. F.; Xu, G. Q. Coordination and reaction mechanism of furan on Ru (001). *J. Chem. Phys.* **1999**, *111* (17), 8068−8076.
(30) Alamillo, R.; Tucker, M.; Chia, M.; Pagan-Torres, Y.; Dumesic, J. The selective hydrogenation of biomass-derived 5-hydroxymethylfurfural using heterogeneous catalysts. *Green Chem.* **2012**, *14* (5), 1413−1419.